Soft Matter

Photopolymerized Microdomains in both Lipid Leaflets Establish Diffusive Transport Pathways across Biomimetic Membranes

Journal:	*Soft Matter*
Manuscript ID	SM-ART-08-2019-001658.R1
Article Type:	Paper
Date Submitted by the Author:	06-Sep-2019
Complete List of Authors:	Makhoul-Mansour, Michelle; University of Georgia, School of Environmental, Civil, Agricultural and Mechanical Engineering El-Beyrouthy, Joyce; University of Georgia, School of Environmental, Civil, Agricultural and Mechanical Engineering Mumme, Hope; Georgia Institute of Technology, Wallace H.Coulter Departement of Biomedical Engineering Freeman, Eric; University of Georgia, School of Environmental, Civil, Agricultural and Mechanical Engineering

ARTICLE

Photopolymerized Microdomains in both Lipid Leaflets Establish Diffusive Transport Pathways across Biomimetic Membranes

Received 00th January 20xx,
Accepted 00th January 20xx

DOI:10.1039/x0xx00000x

Michelle M. Makhoul-Mansour [a] , Joyce B. El-Beyrouthy [a] , Hope L. Mumme [b] and Eric C. Freeman [a]

Controlled transport within a network of aqueous subcompartments provides a foundation for the construction of biologically-inspired materials. These materials are commonly assembeled using the droplet interface bilayer (DIB) technique, adhering droplets together into a network of lipid membranes. DIB structures may be functionalized to generate conductive pathways by enhancing the permeability of pre-selected membranes, a strategy inspired by nature. Traditionally these pathways are generated by dissolving pore-forming toxins (PFTs) in the aqueous phase. A downside of this approach when working with larger DIB networks is that transport is enabled in all membranes bordering the droplets containing the dissolved PFT, instead of occuring exclusively between stained droplets. To rectify this limitation, photopolymerizable phospholipids (23:2 DiynePC) are incorporated within the aqueous phase of the DIB platform, forming conductive pathways in the lipid membranes post-exposure to UV-C light. Notably these pathways are only formed in the membrane if both adhered droplets contain the photo-responsive lipids. Patterned DIB networks can then be generated by controlling the lipid composition within select droplets which creates conductive routes one droplet thick. We propose that the incorporation of photo-polymerizable phospholipids within the aqueous phase of DIB networks will improve the resolution of the patterned conductive pathways and reduce diffusive loss within the synthetic biological network.

Introduction

Living cells coordinate behaviours that are foundational to the natural world, aided by collections of membranous barriers providing an internal structure. These lipid membranes are fundamental cellular elements, delimiting the cells and restricting the undesired diffusion of polar molecules[1]. When transmembrane exchange is necessary for chemical signalling, biosynthesis, or other functions, the lipid bilayers' permeability is altered through membrane-embedded biomolecules acting as pores, channels, and transporters[1-3]. This allows for precise exchanges and spatiotemporal control over the internal composition of each individual cell.

Cellular organisms are able to facilitate complex schemes for communication and adaptation using these mechanisms. These remarkable capabilities have been the focus of bioinspired materials research attempting to reproduce cellular phenomena in engineered structures[4, 5]. While fully reproducing cellular phenomena within the laboratory is unrealistic, it is still possible to replicate select portions of the desired membranous phenomena through the creation of artificial lipid membranes exploiting self-assembly principles.

One approach for recreating lipid membranes is the droplet interface bilayer (DIB) technique (**Figure 1**), establishing biomimetic membranes between lipid-coated aqueous droplets[6-8]. Benefits of this technique include low material consumption, the ability to repeatedly assemble and disconnect multiple lipid bilayers[9, 10], the ability to create asymmetric membranes[11], and the relative ease of implementation. Droplets are deposited in an oil reservoir with lipids dissolved in either phase. After being provided sufficient time for the formation of lipid monolayers at the droplet surfaces, the droplets are brought into contact and lipid bilayers spontaneously form at their interfaces[7, 8, 12]. These membranes may be electrically approximated as a capacitor in parallel with a resistor[13-15] (**Figure 1.a**), and the interfacial membrane dimensions at equilibrium are a function of the monolayer and bilayer tensions[16] (**Figure 1.b**). The DIB technique has been recently widely employed as a reliable platform for the reliable construction of membrane-based materials[17-22].

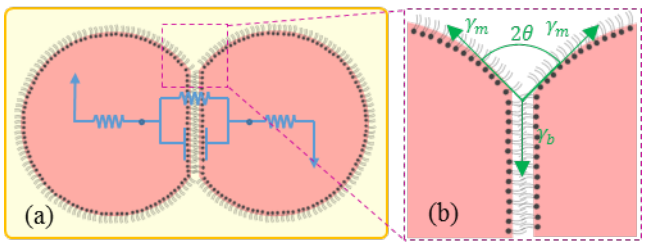

Figure 1. Schematic representation of the droplet interface bilayer (DIB) technique. After being introduced into an oil medium, aqueous droplets acquire a lipid coating referred to as lipid monolayer. As droplets are brought together, oil at their interface is gradually expelled and the lipid bilayer spontaneously forms. A lipid bilayer can be electrically modeled as a capacitor in parallel with a high amplitude resistor. The bilayer interfacial tension is balanced with the two opposing monolayer tensions separated by the angle of contact 2θ.

[a] School of Environmental, Civil, Agricultural and Mechanical Engineering, University of Georgia, Athens, Georgia, 30602, United Sates.
[b] Wallace H. Coulter Department of Biomedical Engineering, Georgia Institute of Technology, Atlanta, Georgia, 30332, United States.

Electronic Supplementary Information (ESI) available including materials, methods used, and additional results: see DOI:10.1039/x0xx00000x

An additional advantage of the DIB technique is the ability to combine multiple membranes into larger networks. Each droplet is separated from neighbouring droplets through either their semi-permeable lipid membranes or the insulating oil. Consequently each droplet may be treated as a separate compartment or domain. Exchange between neighbouring droplets is typically minimized unless the membranes between them are functionalized with transport-enabling biomolecules. This functionalization is typically accomplished through embedded proteins and peptides such as alpha-hemolysin (*αHL*)[18, 23, 24] producing stimuli-responsive soft structures that mimic the versatility of cellular organisms. The collective action of multiple droplets with varying designated functions working in parallel provides the desired emergent properties of the bioinspired materials[25, 26].

PFT-enabled exchange of droplet contents between different compartments within DIB networks has been successfully implemented in various studies[5, 17, 18, 22, 27] . While *αHL* is one of the most reliable agents for creating nanopores in lipid membranes[28] and has been used to create diffusion pathways for membrane-based materials[5, 18], it typically establishes pores in all bilayers surrounding the carrier droplet as depicted in

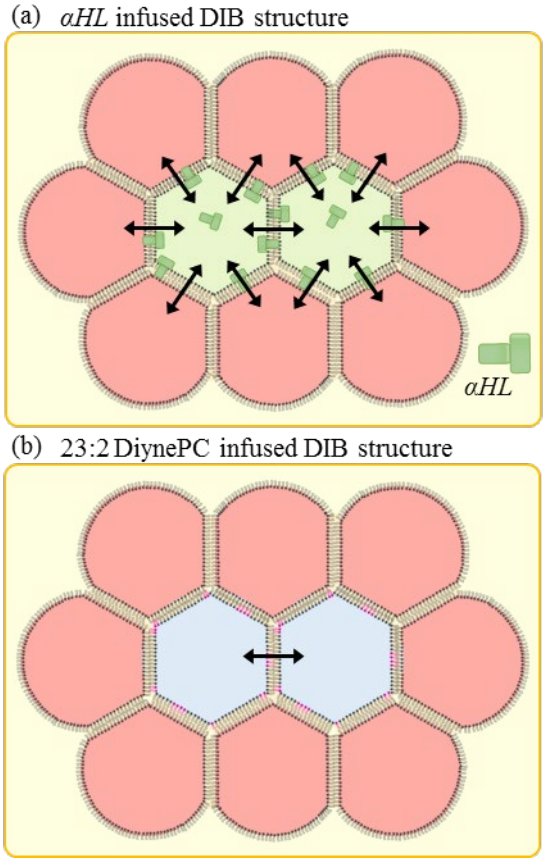

Figure 2. Schematic representation of two different scenarios for the generation of diffusive pathways within DIB structures as indicated by arrows across the interfacial membranes. Red droplets contain DPhPC lipids, green droplets contain DPhPC as well as the pore forming toxin *αHL*, and the blue droplets contain a mixture of DPhPC and 23:2 DiynePC photopolymerizable phospholipids. In (a) when the two central droplets are infused with *αHL*, diffusive pathways are generated in all bordering bilayers. (b) In contrast, if the central droplets are infused with 23:2 DiynePC polymerizable lipids and exposed to UV-C light thus triggering lipid polymerization, diffusive pathways can only be generated between leaflets both containing the DiynePC microdomains.

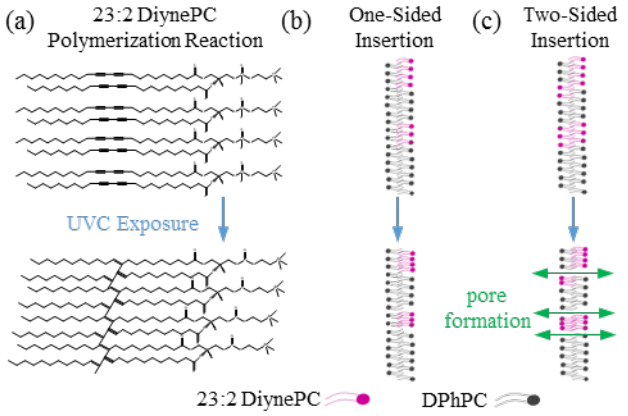

Figure 3. Schematic representations: (a) Cross-linking of 23:2 DiynePC phospholipids after the application of UV-C light for 5 minutes. (b) (c) Cross-linking of 23:2 DiynePC lipids within a lipid bilayer when it was introduced from (b) one side and (c) two sides of the bilayer. As DiynePC polymerized, the lipid chains tightly packed together resulting in the formation of structural pores within the lipid bilayer whenever polymerizable lipids were present on both sides as shown in (c). Pores in this case are a result of polymerizable lipids tightly packing together forming discontinuities in the molecular distribution at the monolayer and bilayer levels. Owing to the positioning of the diacetylene groups within each lipid molecule and to the ordered alignment polymerization condition, no cross-leaflet polymerization is anticipated. Polymerization is constricted to occur between molecules present on the same leaflet.

Figure 2.a. Unintentional diffusive exchange occurs as a result where multiple membranes are functionalized with the pore[10, 29, 30].

Naturally occurring membrane-bound transporters such as *αHL* span the entire thickness of the membrane interior. This is unsurprising given their intended role, but leads to this previously noted shortcoming in diffusive loss when reassembling these materials. An ideal replacement for these pores would only enable exchange between droplets that both share a common characteristic, eliminating the unintentional diffusive exchange by restricting how the channels are constructed such as in **Figure 2.b**. This replacement requires an alternative approach for modifying the membrane permeability.

The permeability of a lipid membrane is also influenced by the membrane's lipid composition. When multiple types of lipids are incorporated within model bilayers, their suprastructure or lateral organization is not random[31] and is viewed in the context of the fluid mosaic model[32]. Bilayers containing a mixture of different lipids often exhibit an amphiphilic self-organization phenomenon[31-35] that helps minimize unfavourable interactions between dissimilar lipids[36, 37]. Furthermore the presence of coexisting lipid microdomains or phases has been observed to enhance transmembrane diffusion[38, 39], and these microdomains may be created through photoresponsive lipids. 23:2 DiynePC [DC (8,9) PC], also known as 1,2-bis(10,12-tricosadiynoyl)-sn-glycero-3 phosphocholine, is a synthetic phospholipid containing two diacetylene groups. The diacetylene groups render this lipid polymerizable through UV-C exposure similar to various types of other synthetic polymerizable lipids (optimized at 254 nm irradiation wavelength[35, 40-44]). When diacetylene-containing lipid compounds are arranged in a highly ordered arrays[35, 45], UV-C light causes the two conjugated triple bonds of the lipid

monomers to be replaced in the final polymer by an alternating double-bonded and triple-bonded conjugated structure, linking the lipids together and forming stable microdomains within the membrane[46] as illustrated in **Figure 3**. This polymerization mechanism occurs when lipids are present at a condensed and highly ordered (corresponding to a correct alignment of the diacetylene groups) state[47].

The polymerization of UV-sensitive lipids within liposomes allowed for the release of their contents across the membrane, including calcein, HPPH (2-(1-Hexyloxyethyl)-2-devinyl pyropheophorbide-a) and even doxorubicin[48, 49], demonstrating enhanced membrane permeability through photopolymerization. The incorporation of photopolymerizable lipids in DIBs was first suggested by Punnamaraju *et al.*[48, 50] as a method for studying phototriggered drug delivery systems *in vitro*. The introduction of the photosensitive lipids into the oil phase of a DIB was shown to allow for successful calcein diffusion across the membrane after UV-C exposure and formation of transmembrane pores[50] in agreement with previously reported results.

The cause of the increased membrane permeability when 23:2 DiynePC lipids are incorporated is expected to require the presence of polymerized microdomains in both leaflets and is suggested to be the result of a transmembrane coordination of defects. Since the DIB approach allows for the creation of asymmetric membranes by varying the lipid composition within the droplets, it is possible to limit the formation of the transmembrane defects as a function of the droplet lipid compositions. The selective dissolution of DiynePC in the aqueous phase would only establish transmembrane defects between droplets that both contain the DiynePC microdomains (**Figure 3.b.**) thus limiting droplet-droplet exchange to compatible droplets. This would allow for tailored membrane permeability through membrane structure and asymmetry.

These phototriggered diffusive pathways may be established within larger DIB structures, only creating pores between droplets with similar compositions and avoiding the issues presented by *αHL* and similar PFTs. Light-sensitive DIB networks have been explored previously in the literature[4, 27, 51], altering the membrane characteristics either through bacteriorhodopsin or through the *in vitro* transcription/translation (IVTT) of *αHL* triggered through UV exposure. In this work, UV-C exposure is used to modify properties of the membranes by inducing an increased membrane permeability through the formation of photo-polymerized domains within the leaflets.

In this manuscript we demonstrate that DiynePC-enabled diffusion only occurs in bilayers that incorporate polymerizable lipids within both leaflets as depicted in **Figure 3**. The qualities of DIBs formed with different ratios of added polymerizable lipids and different oils are assessed using tensiometry and their induced change in conductance are measured through electrophysiology. In light of these results, a suitable aqueous-lipid and oil-lipid mixtures combination is then determined and used to form larger 2D bilayer structures. The advantages of the phototriggered diffusive pathways are showcased by comparing the activity of *αHL* and polymerizable DiynePC in similar DIB structures. Finally, the diffusive capabilities of these bilayers is displayed through calcein diffusion.

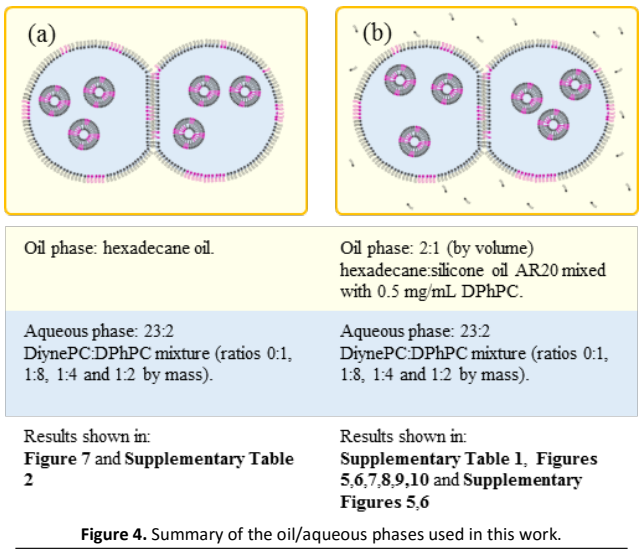

Figure 4. Summary of the oil/aqueous phases used in this work.

Materials and Methods

Detailed protocols for solution preparation and experimental methodologies may be found in the **Supplementary Information**. A brief overview of these approaches is provided below.

Aqueous solutions containing varying ratios of DiynePC and 1,2-diphytanoyl-sn-glycero-3-phosphocholine (DPhPC) were prepared[52]. Droplets of these solutions were injected into oil reservoirs using microinjectors. This oil was either a 2:1 hexadecane:silicone oil AR20 mixture containing dissolved DPhPC at 0.5 mg/mL or hexadecane without lipids (**Figure 4**).

Monolayer surface tension measurements were taken using pendant drop tensiometry with a custom stage (illustrated in **Supplementary Figure 1**) and the open-source software OpenDrop[53].The kinetics of monolayer formation, monolayer tension at equilibrium, and influence of UV-C exposure were tracked as a function of the ratio of DiynePC:DPhPC within the aqueous phase. Changes in the equilibrium energy per area was tracked as evidence of successful photo-polymerization of the interface.

Membrane characterization was accomplished through electrophysiology. Droplets were directly deposited onto silver/silver-chloride (Ag/AgCl) electrodes coated in agarose within an appropriately grounded Faraday cage on a microscope stage and connected to electrophysiology equipment. Voltage was applied across the membrane using function generators with the patch-clamp amplifier in voltage-clamp mode, and the membrane response was recorded and exported for post-processing to extract the net membrane capacitance and conductance. Micrographs of the adhered droplet geometry were then combined with the electrical recordings to produce the membrane specific capacitance and conductance, or the capacitance and conductance per membrane area.

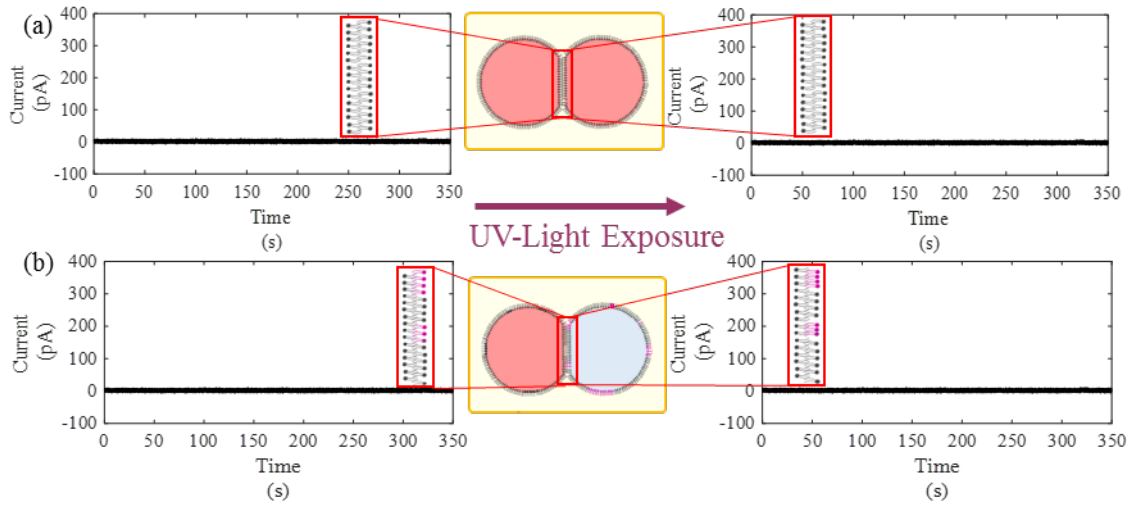

Figure 5. Current traces obtained for a constant applied voltage of +100 mV before and after application of UV-C light for 5 minutes. The red droplets contain DPhPC dissolved at 2.5 mg/mL and blue droplets contain 1:4 mixture of 23:2 DiynePC:DPhPC dissolved at 2.5 mg/mL. The solvent is 2:1 hexadecane:silicone oil AR20 0.5 mg/mL DPhPC oil-lipid mixture. In (a) the DIB is formed between two aqueous droplets only containing DPhPC. No pore formation is noted after the application of UV-C, and the membrane remains highly resistive. In (b) the DIB is formed between two aqueous droplets containing polymerizable and non-polymerizable phospholipids. No pore formation is noted after the application of UV-C. Similar traces were observed when the ratio of polymerizable to non-polymerizable lipids were 1:2 and 1:8 by mass respectively and when hexadecane alone was used as an external phase as well. All measurements were recorded in voltage clamp mode at a sampling frequency of 10 kHz and filtered at 1 kHz (using the embedded low-pass Bessel filter −80 dB/decade). Post-acquisition, data was filtered at 500 Hz using a fourth-order Butterworth low-pass filter in MATLAB.

The solutions were cured either prior to droplet formation or *in situ* using a 254 nm UV-C mercury lamp for 5 minutes. UV-C enabled transmembrane exchange was characterized in single adhered droplet pairs and networks of adhered droplets for all cases. When droplet networks were desired, the droplets were deposited within an acrylic egg crate substrate to hold the droplets in place[14]. Diffusion of calcein was tracked using fluorescent microscopy and ImageJ.

Results and Discussion

Membrane Conductance with Asymmetric/Symmetric Distribution of 23:2 DiynePC Polymerizable Lipids

Photopolymerizable lipids were tested for enabling diffusive transport between adjacent droplets. Transmembrane diffusion is hypothesized to occur as a result of photopolymerized DiynePC microdomains [50] interactions (**Figure 3**) across opposing monolayers. The differences between asymmetric and symmetric distributions of the UV-sensitive lipid was not reported in the literature, but the transport should only be enabled when DiynePC is present in both leaflets in contrast to the behaviour of *αHL* shown in **Supplementary Figure 3.** This requirement for symmetric distributions of the phospholipids to enable transport is similar the mechanics of gramicidin dimers shown in **Supplementary Figure 4**. However, DiynePC is preferred over gramicidin since it is not cation selective and may be further controlled by UV-C exposure. As a baseline point of reference, DIBs containing only the non-polymerizable DPhPC phospholipids were first tested. Current traces with a constant voltage before and after UV-C light exposure are shown in **Figure 5.a.** where no conductive currents are reported demonstrating that the induced defects are not functions of UV-C exposure alone. Next the symmetric/asymmetric DiynePC:DPhPC studies were conducted as shown in **Figure 5.b.** for asymmetric bilayers and **Figure 6** for symmetric bilayers with different ratios of the polymerizable lipids. As suggested by the previous hypothesis and confirmed in **Figure 5** and **Figure 6**, the enhanced membrane permeability only occurs when both adhered droplets contain photopolymerized DiynePC microdomains.

Several trends are noted. First, when the photopolymerizable lipids are present only on one side of the bilayer, no changes in membrane conductance are observed (**Figure 5.b**). This was consistent for all concentrations of the photopolymerizable lipids and all oils. Second, the symmetric membranes exhibited negligible conductance prior to UV-C exposure, even with greater ratios of DiynePC:DPhPC. All cases with symmetric distributions of DiynePC shown in **Figure 6** exhibit drifting changes in conductance as the rafts in both leaflets align and separate across the membrane. Similar changes in membrane conductance were observed whether the solutions were polymerized *in situ* after membrane formation or prior to droplet deposition. Electrical recordings during photopolymerization cannot be provided because of the high noise levels generated by the UV-C source[50]. The photopolymerized DIBs exhibit stability comparable to unmodified DPhPC DIBs and typically lasted for the maximum duration of an experiment (>6 hours) with an applied 100 mV DC voltage. Finally, while the membrane conductance varies with respect to time dependent on domain alignment, the measured increases in conductance generated by DiynePC are considerably larger than the increases provided by *αHL* (**Supplementary Figure 3**).

Cyclic Voltammetry Results

Next cyclic voltammetry was used to further compare the conductive current induced by DiynePC with different lipid ratios. Lipid bilayers formed using traditional non-polymerizable phospholipids such as DPhPC are not expected to exhibit notable current-voltage dependent behaviour relative

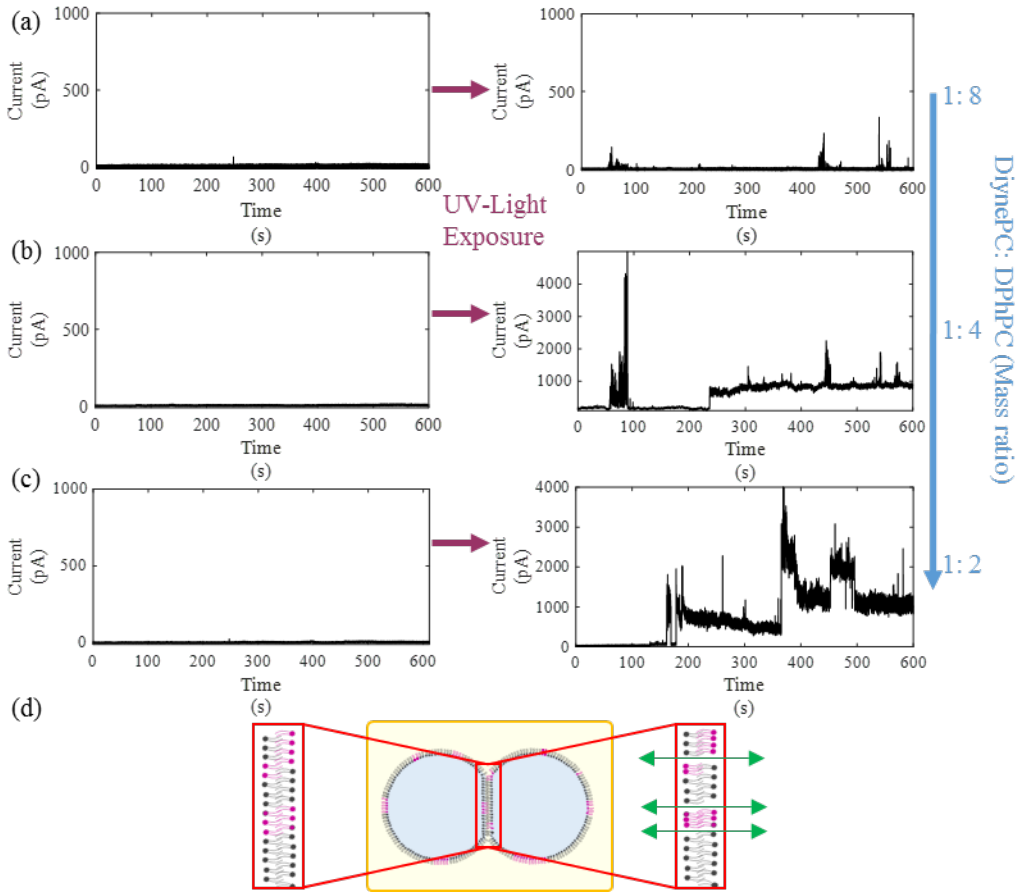

Figure 6. Current traces obtained for a constant applied voltage of +100 mV before and after application of UV-C light for 5 minutes. The DIBs are formed between two aqueous droplets containing polymerizable and non-polymerizable phospholipids (23:2 DiynePC and DPhPC) dissolved at a concentration of 2.5 mg/ml in a 2:1 hexadecane:silicone oil AR 20 0.5 mg/mL DPhPC oil-lipid mixture. The ratio of polymerizable to non-polymerizable lipids by mass was (a) 1:8, (b) 1:4, and (c) 1:2. Polymerizable lipids were introduced form both sides of the bilayer. Similar trends can be observed when Hexadecane oil is used as an external phase. (d) Shows a schematic representation of the formed bilayer pre and post UV-C curing. All measurements were recorded in voltage clamp mode at a sampling frequency of 10 kHz and filtered at 1 kHz (using the embedded low-pass Bessel filter −80 dB/decade). Post-acquisition, data was filtered at 500 Hz using a fourth-order Butterworth low-pass filter in MATLAB.

to composite lipid membranes with incorporated peptides or more specifically pores[21, 24]. **Figure 7** shows current *vs.* voltage traces obtained for bilayers containing the polymerized lipids. The bilayer containing polymerizable lipids exhibits an increase in conductance as the ratio of the DiynePC:DPhPC is augmented. This increase in conductance is likely caused by the increased probability of the polymerized lipid microdomains co-locating within the bilayer as the amount of DiynePC is increased, thus inducing localized lipid packing defects. This graph additionally shows that the 1:8 DiynePC:DPhPC mass ratio does not reliably increase the membrane conductance compared to higher lipid ratios. Lipid mass ratios of 1:4 and 1:2 DiynePC:DPhPC respectively exhibit membrane conductance behaviours similar to those of pores and peptides[5].

DIB Properties

DIB properties including angle of contact, monolayer tension, bilayer tension, energy of adhesion, bilayer thickness, specific conductance, and specific capacitance were evaluated for bilayers formed in the hexadecane:silicone oil AR20 0.5 mg/mL DPhPC lipid-oil mixture (described in more details in the Materials section) where 23:2 DiynePC has been symmetrically introduced into the aqueous phase at different concentrations. This oil mixture has been selected as it enables greater droplet-droplet adhesion[54] as well as an ease in network creation by reducing gravitational influences[54]. DPhPC was dissolved in the oil mixture (lipids-out) and mixtures of DiynePC:DPhPC were

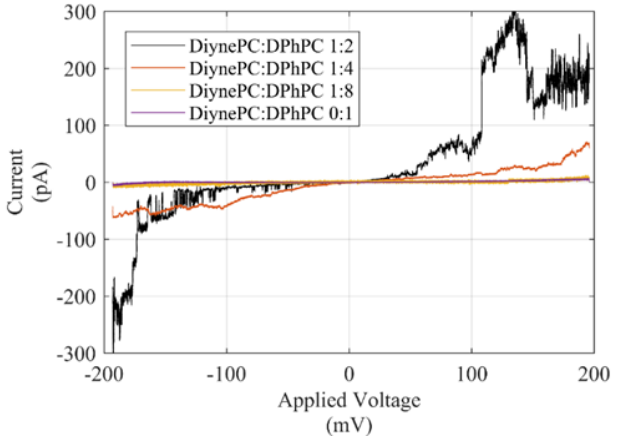

Figure 7. Current-voltage plots demonstrating pores formed post UV-C curing for different concentrations of polymerizable phospholipids (2.5 mg/ml in total in the aqueous phase) within the 2:1 hexadecane:silicone oil AR20 containing 0.5 mg/mL DPhPC lipid-oil mixture. A 4 mV/s voltage-sweep for these bilayers was performed and current responses recorded. All measurements were recorded in voltage clamp mode at a sampling frequency of 10 kHz and filtered at 1 kHz (using the embedded low-pass Bessel filter −80 dB/decade). Post-acquisition, data was filtered at 500 Hz using a fourth-order Butterworth low-pass filter in MATLAB.

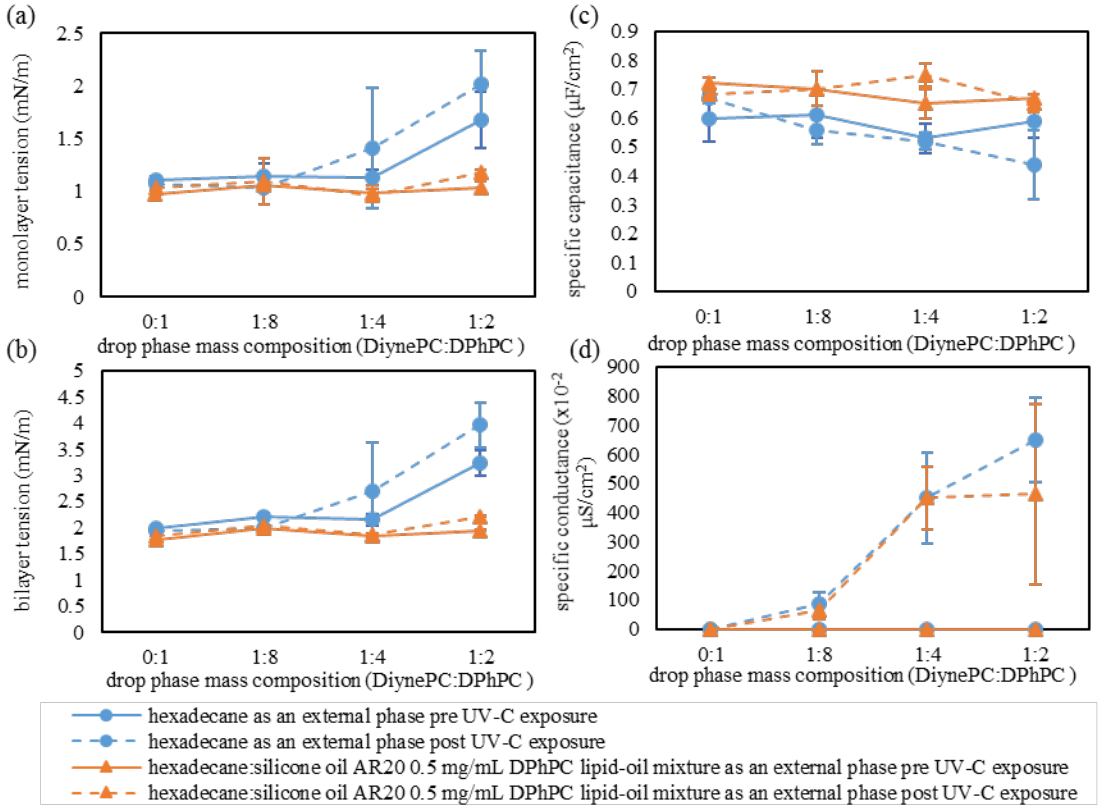

Figure 8. Measurement of the properties of lipid bilayers in hexadecane as well as 2:1 hexadecane:silicone oil AR20 DPhPC oil-lipid mixture for increasing concentrations of polymerizable lipids dissolved in the aqueous phase (2.5 mg/ml total) pre and post UVC exposure for 5 minutes. (a) shows the monolayer tension (mN/m), (b) shows the bilayer tension (mN/m) ,(c) shows the bilayer's specific capacitance (μF/cm²) while (d) shows the bilayer's specific conductance (x10⁻² μS/cm²).

selectively dissolved in the aqueous solutions to enable to formation of diffusive bridges. Dissolving DPhPC in both the aqueous and oil phases has been shown to enhance the DIB network stability[18], and the 2:1 hexadecane:silicone oil AR20 DPhPC is well-suited for lipid-out experiments. DiynePC was introduced only from the aqueous phase and was not dissolved in the oil phase, ensuring the ability to produce asymmetric membranes when necessary (**Figure 4.b**).

Supplementary Table 1 includes measurements of the interfacial properties formed in a 2:1 hexadecane:silicone oil AR20 mixture with 0.5 mg/mL DPhPC in the continuous phase as used for the creation of droplet networks, and select trends are plotted in **Figure 8**. The DIBs specific capacitance as well as the monolayer tensions show no noticeable change pre and post polymerization for different introduced proportions of DiynePC. Meanwhile, as shown in the same table, the values for the contact angles show some change compared to a control case where no polymerizable lipids are present. However, there is not a clear relationship between the variation in the angle of contact and the proportion of 23:2 DiynePC introduced into the bilayer. These measurements are in a reasonable agreement with previously reported results for lipid bilayers formed through the DIB technique[54].

A clear change in membrane conductance pre and post UV-C exposure is demonstrated as measured by the specific conductance or conductance per area (**Figure 8.d**). Specific conductance is reported since the membrane dimensions vary with the amount of DiynePC. Bilayers that did not contain polymerizable lipids show no increase in their specific conductance. Small changes observed after UV irradiation in the case of DPhPC alone have been attributed in the literature with some disturbances caused by UV light or small motions among lipid molecules caused by formation of gauche defects[55]. Meanwhile, membranes containing DiynePC show a clear increase in their specific conductance post photo-polymerization. As expected from the cyclic voltammetry results, the specific conductance increases with the DiynePC:DPhPC ratio.

While dissolving DPhPC in the oil phase does not eliminate the influence of DiynePC on the membrane properties, it also does not isolate the influence of DiynePC on the interfacial properties as demonstrated in **Figure 8.a** and **Figure 8.b** as well as **Supplementary Table 1**. This was addressed by measuring these interfacial properties in hexadecane alone with no dissolved lipids in the oil (**Figure 4.a**). These experiments, summarized in **Figure 8** and **Supplementary Table 2** show more decisive trends in the membrane parameters, highlighting the influence of DiynePC. A remarkable decrease in the angle of contact as reported by the bilayer and monolayer tensions (**Figure 8.a-b**) is noted prior to UV-C exposure as the ratio of DiynePC:DPhPC increases from 0:1 to 1:2. Post UV-C treatment, the angle of contact decreases further, suggesting the possible creation of microdomains within the monolayer. Clear changes in the specific conductance of the membrane pre and post UV-C

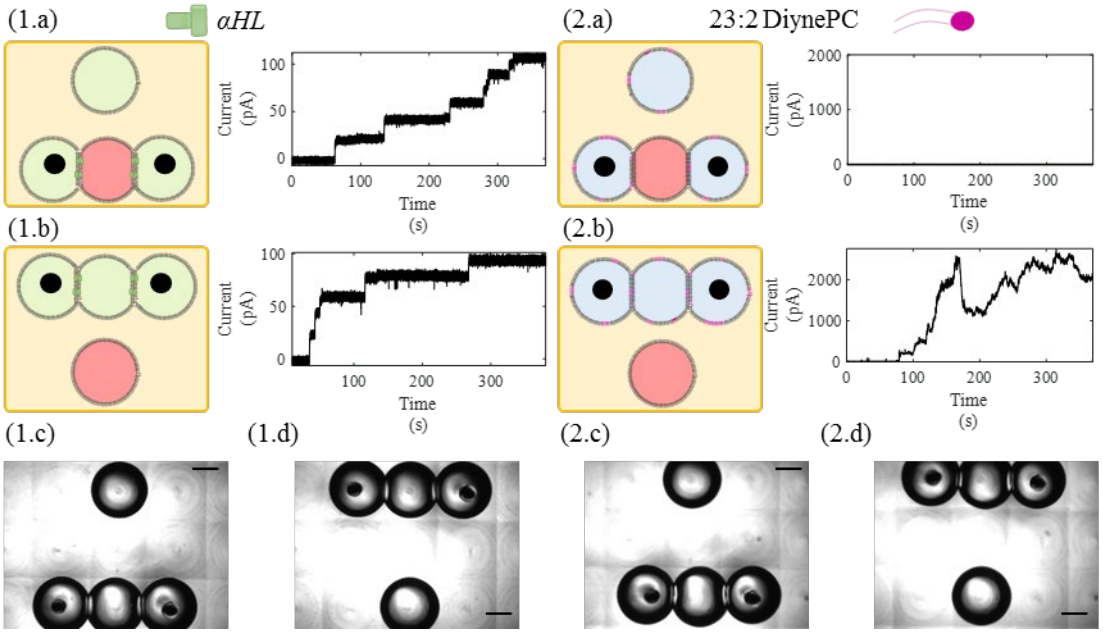

Figure 9. Current traces obtained for a constant applied voltage (+100 mV) and illustrating the properties of *αHL* and DiynePC. In both cases the red droplets contain only 2.5 mg/ml of DPhPC. Droplets are dispersed in a 2:1 hexadecane:silicone DPhPC lipid oil mixture to facilitate bilayer formation. A +200 mV DC potential is applied between the electrodes, resulting in approximately +100 mV per membrane. (1) The green droplets contain 1.25 µg/mL of dissolved *αHL*. Both droplet configurations shown in (1.a) and (1.b) result in the formation of a conductive pathway across the entire network since *αHL* is not required to insert from both sides of the membrane for pore formation. (2) Current traces obtained post application of a UV-C light for 5 minutes, illustrating the behaviour of polymerized 23:2 DiynePC mixtures. The blue droplets contain a 1:4 mass ratio 23:2 DiynePC:DPhPC mixture dissolved at a total concentration of 2.5 mg/ml. In (2.a), the OFF configuration was switched by having a red droplet placed between two blue input droplets, stopping exchange across both membranes. In (2.b), the micro switch was turned to the ON configuration by moving the blue input droplets connected to the acquisition system so that all droplets containing polymerizable lipids were aligned in contrast with the case shown in (1.a) and (1.b). (1.c), (1.d), (2.c) and (2.d) show the images acquired for (1.a), (1.b), (2.a) and (2.b) respectively. All measurements were recorded in voltage clamp mode at a sampling frequency of 10 kHz and filtered at 1 kHz (using the embedded low-pass Bessel filter −80 dB/decade). Post-acquisition, data was filtered at 500 Hz using a fourth-order Butterworth low-pass filter in MATLAB. Scale bars represent 400 µm.

exposure are observed, varying with the DiynePC:DPhPC ratio (**Figure 8.d**). It is worth noting that in **Figure 8.c**, **Supplementary Table 1,** and **Supplementary Table 2**, the bilayers' specific capacitance do not exhibit definitive trends and fall within reported ranges for DPhPC membranes[54].

While the 1:2 DiynePC:DPhPC droplet formulation allows for a highly permeable membrane (**Figure 8.d**) and shows properties that are in agreement with ranges for bilayer properties previously reported in the literature (**Figure 8.c**)[54, 56], this mixture poses additional challenges for membrane formation. When using the 1:2 DiynePC:DPhPC lipid mass ratio an applied +150 mV DC voltage was necessary to induce bilayer formation through electrostatic compression even when using the 2:1 hexadecane:silicone oil AR20 DPhPC mixture. After formation, the membranes retained their integrity and the droplets no longer required the external voltage to remain adhered together. Still, this renders the construction of a DIB network more challenging as voltage must be applied to each droplet pair to induce bilayer formation. This drawback was not observed for the 1:8 and 1:4 DiynePC:DPhPC mixtures. The differences between the two solvents is summarized in **Figure 4**. The hexadecane solvent without dissolved lipids exhibits a slightly higher change in the specific conductance relative to the 2:1 hexadecane:silicone oil AR20 mixture with 0.5 mg/mL DPhPC (**Figure 8.d**). However this value is a specific conductance or conductance per membrane area, and the reduction in contact angle and energy of adhesion with hexadecane alone (**Supplementary Table 2**) will also diminish the net gain in membrane conductance. Furthermore the use of the 2:1 hexadecane:silicone oil AR20 solvent reduces gravitational influences on the droplets and is preferred for network formation. From these experimental observations the best solution is to mix 23:2 DiynePC with DPhPC at a mass ratio of 1:4 and deposit these droplets into the 2:1 hexadecane:silicone oil AR20 DPhPC lipid-oil mixture to form stable DIB structures where the UV-sensitive lipids can induce droplet-droplet exchange after UV-C exposure. The remaining experimental results use this formulation.

Phototriggered Diffusive Pathways in DIB Networks

DiynePC may be used for phototriggered diffusive pathways through asymmetric distributions of the light-sensitive lipid. These diffusive pathways are only enabled when both droplets contain the UV-sensitive lipids, providing a greater degree of control over the diffusive transport and exploiting the ability to simply fabricate asymmetric membranes using the DIB technique.Transport is feasible across droplet chains after UV-C exposure only when all of the connected droplets contain DiynePC. **Figure 9.2** shows a micro-switch formed using four droplets. The droplet marked in red only contains non-polymerizable phospholipids while the ones marked in blue contain the 1:4 DiynePC:DPhPC mixture. **Figure 9.2.a** shows the OFF configuration, with the anchor droplets (droplets connected to the electrodes) being connected to the red droplet. No pores can be formed through this configuration as polymerizable lipids are only present on one side in each of the

two bilayers and the measured current remains negligible as expected. If *αHL* had been used instead of photopolymerized lipids as shown in **Figure 9.1**, the switch would have generated a conductive pathway in either configuration (**Figure 9.1.a** and **Figure 9.1.b** respectively). **Figure 9.2.b** shows the ON configuration that occurs when the anchor droplets are moved up to form two bilayers with the third photo-sensitive droplet sandwiched in between. As anticipated, pores were formed once 23:2 DiynePC was present on both sides of each bilayer. **Supplementary Figure 5** and **Supplementary Figure 6** show larger photo-sensitive DIB structures with conductive pathways generated between 4 then 6 polymerized membranes. Both figures show that the conductive pathway is not generated unless all droplets containing polymerized lipids align and form defects within the membranes separating the droplets.

Calcein Diffusion across a Single DIB

An advantage of DiynePC is its ability to facilitate the diffusion of larger molecules across the membrane. This is examined here by tracking the diffusion of calcein between two droplets using fluorescent microscopy. **Figure 10** shows the diffusion of calcein across bilayers with incorporated polymerized lipids. Calcein is encapsulated in a donor droplet at a concentration of 0.25 mg/ml. When donor droplets containing polymerized 23:2 DiynePC along with DPhPC in a 1:4 mass ratio are coupled with an acceptor droplet containing DPhPC only, no significant release of calcein across the membrane is observed (**Figure 10.a**). This is because the distribution of DiynePC within the membrane is asymmetric, and transmembrane defects are not present as shown in **Figure 5.a**. When DiynePC was present in both the donor and receptor droplets as shown in **Figure 10.b**, calcein was capable of diffusing across the bilayer. The diffusive exchange is quantified as a function of the ratio of fluorescent intensities of the droplets. The ratio of the fluorescent intensity of the acceptor droplet vs. the donor droplet increased in this case whereas it remained constant in the control case (shown in **Figure 10.a**). The release of calcein in **Figure 10.b**, can be attributed to the enhanced permeability of the bilayer upon the symmetric introduction of C23 polymerizable lipids. This confirms previous results obtained in this work the selective introduction of DiynePC in the aqueous phase of DIBs. Conductive pores can only be created between droplets that share the same composition, and droplet-droplet exchange is limited to droplets with similar lipid compositions.

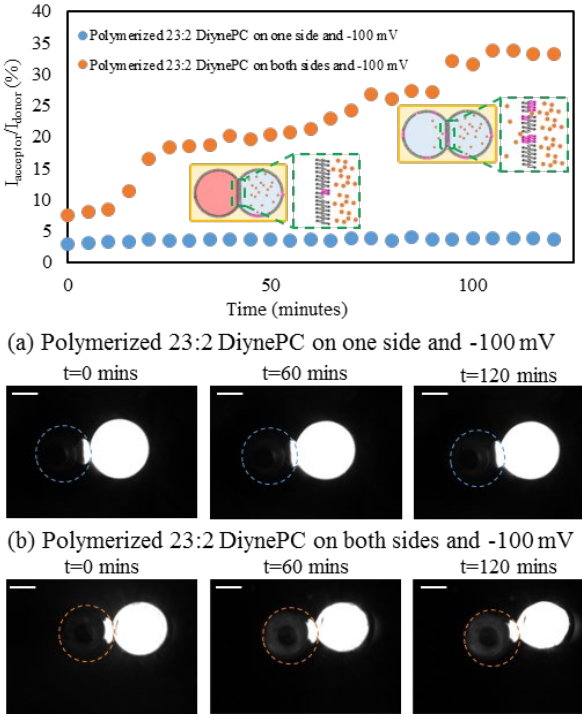

Figure 10. Release of calcein from donor droplet (right droplet corresponding to the reference side of the bilayer) to the acceptor droplet (left droplet). The plot shows the percentage of calcein fluorescence vs time in the acceptor droplet ($I_{acceptor}$) vs the donor (I_{donor}) droplet for the four experimental cases. (a), (b), (c) and (d) show the respective fluorescence images for the DIBs. Bright areas indicate the presence of calcein while dark areas do not contain calcein. In all experimental cases, a -100 mV was being applied and the 2:1 hexadecane:silicone DPhPC oil-lipid mixture was used. (a) Images acquired for the control case where the donor droplet contained pre-polymerized 23:2 DiynePC (as well as DPhPC at a mass ratio of 1:4) and calcein (at a concentration of 0.25 mg/ml) while the acceptor droplet contained non-polymerizable lipids only (DPhPC). (b) Both droplets contain pre-polymerized 23:2 DiynePC (as well as DPhPC at a mass ratio of 1:4) but calcein is only present in the donor droplet at a concentration of 0.25 mg/ml. Scale bars represent 200 µm.

Conclusion

Herein we present a new application for UV-polymerizable lipids within the DIB platform. Our research shows that when diacetylene-enabled lipids are incorporated and polymerized on both leaflets of a lipid membrane, pores are produced within the membrane confirming previous hypotheses on the mechanics of DiynePC-aided transmembrane diffusion[48, 50, 57]. A key advantage of this approach is the requirement for DiynePC in both leaflets for enhanced membrane permeability. This approach exploits the capability to create asymmetric membranes using the DIB technique, producing patterned diffusive pathways within the droplet network. When compared to pores formed by *αHL* and gramicidin, defects induced by the UV-triggered lipid packing alteration are advantageous due to their symmetry requirements for conductance and their non-selectivity for transported molecules. Our approach reduces unwanted diffusion by patterning diffusive pathways in droplet networks through UV-C exposure and lipid microdomains.

Conflicts of interest

There are no conflicts to declare.

Acknowledgements

The authors graciously acknowledge support from the National Science Foundation (NSF) under grant # 1537410.

Notes and references

1. B. Apellániz, J. L. Nieva, P. Schwille and A. J. García-Sáez, *Biophysical journal*, 2010, **99**, 3619-3628.

2. D. S. Cafiso, *Annual Reviews-Biophysical Biolmolecular Structures* 1994, **23**, 141-165.
3. O. Andersen, *Biophysical journal*, 1983, **41**, 119-133.
4. M. J. Booth, V. R. Schild, S. J. Box and H. Bayley, *Scientific reports*, 2017, **7**, 9315.
5. E. J. Challita, J. S. Najem, R. Monroe, D. J. Leo and E. C. Freeman, *Scientific reports*, 2018, **8**.
6. J. Bibette, F. L. Calderon and P. Poulin, *Reports on Progress in Physics*, 1999, **62**, 969.
7. K. Funakoshi, H. Suzuki and S. Takeuchi, *Analytical chemistry*, 2006, **78**, 8169-8174.
8. H. Bayley, B. Cronin, A. Heron, M. A. H. W. L. H. R. Syeda, J. Thompson and M. Wallace, *Royal Society of Chemistry* 2008, **4**, 1191-1208.
9. R. Syeda, M. A. Holden, W. L. Hwang and H. Bayley, *J Am Chem Soc*, 2008, **130**, 15543-15548.
10. E. J. Challita and E. C. Freeman, *Langmuir*, 2018, **34**, 15166-15173.
11. G. Taylor, M.-A. Nguyen, S. Koner, E. Freeman, C. Patrick Collier and S. A. Sarles, *Biochimica et Biophysica Acta (BBA) - Biomembranes*, 2018, DOI: https://doi.org/10.1016/j.bbamem.2018.07.001.
12. G. A. Venkatesan, J. Lee, A. B. Farimani, M. Heiranian, C. P. Collier, N. R. Aluru and S. A. Sarles, *ACS-Langmuir*, 2015, **31**, 12883-12893.
13. M. A. Creasy, E. C. Freeman, M. K. Philen and D. J. Leo, *Journal of Intelligent Material Systems and Structures*, 2014, **26**, 921-930.
14. E. C. Freeman, A. B. Farimani, N. R. Aluru and M. K. Philen, *Biomicrofluidics*, 2015, **9**, 064101.
15. W. L. Hwang, M. A. Holden, S. White and H. Bayley, *Journal of the American Chemical Society*, 2007, **129**, 11854-11864.
16. S. S. Dixit, A. Pincus, B. Guo and G. W. Faris, *ACS-Langmuir*, 2012, **28**, 7442-7451.
17. G. Villar, A. D. Graham and H. Bayley, *Science*, 2013, **340**, 48-52.
18. T. Wauer, H. Gerlach, S. Mantri, J. Hill, H. Bayley and K. T. Sapra†, *ACS-NANO*, 2014, **8**, 771–779.
19. M. Bayoumi, H. Bayley, G. Maglia and K. T. Sapra, *Sci Rep*, 2017, **7**, 45167.
20. S. Ma, N. Mukherjee, E. Mikhailova and H. Bayley, *Advanced Biosystems*, 2017, **1**.
21. S. A. Sarles and D. J. Leo, *Lab Chip*, 2010, **10**, 710-717.
22. Y. Elani, A. Gee, R. V. Law and O. Ces, *Chemical Science*, 2013, **4**, 3332.
23. M. A. Holden and H. Bayley, *Journal of the American Chemical Society*, 2005, **127**, 6502-6503.
24. S. Punnamaraju and A. J. Steckl, *Langmuir*, 2011, **27**, 618-626.
25. G. Maglia, A. J. Heron, W. L. Hwang, M. A. Holden, E. Mikhailova, Q. H. Li, S. Cheley and H. Bayley, *Nature Nanotechnology*, 2009, **4**, 437-440.
26. M. A. Holden, D. Needham and H. Bayley, *J Am Chem Soc*, 2007, **129**, 8650-8655.
27. M. J. Booth, V. R. Schild, A. D. Graham, S. N. Olof and H. Bayley, *Sci Adv*, 2016, **2**, e1600056.
28. S. Renner, A. Bessonov and F. C. Simmel, *Applied Physics Letters*, 2011, **98**, 083701.
29. J. E. Gouaux, O. Braha, M. R. Hobaugh, L. Song, S. Cheley, C. Shustak and H. Bayley, *Proceedings of the National Academy of Sciences*, 1994, **91**, 12828-12831.
30. L. Song, M. R. Hobaugh, C. Shustak, S. Cheley, H. Bayley and J. E. Gouaux, *Science*, 1996, **274**, 1859-1865.
31. B. A. Armitage, D. E. Bennett, H. G. Lamparski and D. F. O'Brien, in *Biopolymers Liquid Crystalline Polymers Phase Emulsion*, Springer, 1996, pp. 53-84.
32. T. Okazaki, Y. Tatsu and K. Morigaki, *Langmuir*, 2009, **26**, 4126-4129.
33. D. F. O'Brien, B. Armitage, A. Benedicto, D. E. Bennett, H. G. Lamparski, Y.-S. Lee, W. Srisiri and T. M. Sisson, *Accounts of chemical research*, 1998, **31**, 861-868.
34. M. D. Collins, *Biophysical journal*, 2008, **94**, L32-L34.
35. J. Leaver, A. Alonso, A. A. Durrani and D. Chapman, *Biochimica et biophysica acta (BBA)-biomembranes*, 1983, **732**, 210-218.
36. D. Lingwood and K. Simons, *Science*, 2010, **327**, 46-50.
37. K. Simons and W. L. Vaz, *Annu. Rev. Biophys. Biomol. Struct.*, 2004, **33**, 269-295.
38. S. H.-w. Wu and H. M. McConnell, *Biochemical and biophysical research communications*, 1973, **55**, 484-491.
39. L. Cruzeiro-Hansson and O. G. Mouritsen, *Biochimica et Biophysica Acta (BBA)-Biomembranes*, 1988, **944**, 63-72.
40. D. S. Johnston, S. Sanghera, M. Pons and D. Chapman, *Biochimica et Biophysica Acta (BBA)-Biomembranes*, 1980, **602**, 57-69.
41. K. Morigaki, T. Baumgart, A. Offenhäusser and W. Knoll, *Angewandte Chemie International Edition*, 2001, **40**, 172-174.
42. K. Morigaki, T. Baumgart, U. Jonas, A. Offenhäusser and W. Knoll, *Langmuir*, 2002, **18**, 4082-4089.
43. J. H. Georger, A. Singh, R. R. Price, J. M. Schnur, P. Yager and P. E. Schoen, *Journal of the American Chemical Society*, 1987, **109**, 6169-6175.
44. F. J. Freeman, J. A. Hayard and D. Chapman, *Biochemical Society Transactions*, 1987, **15**.
45. G. Wegner, *Die Makromolekulare Chemie: Macromolecular Chemistry and Physics*, 1972, **154**, 35-48.
46. J. A. Hayward and D. Chapman, *Biomaterials*, 1984, **5**, 135-142.
47. U. Jonas, K. Shah, S. Norvez and D. H. Charych, *Journal of the American Chemical Society*, 1999, **121**, 4580-4588.
48. A. Yavlovich, A. Singh, S. Tarasov, J. Capala, R. Blumenthal and A. Puri, *Journal of thermal analysis and calorimetry*, 2009, **98**, 97-104.
49. J. Sine, C. Urban, D. Thayer, H. Charron, N. Valim, D. B. Tata, R. Schiff, R. Blumenthal, A. Joshi and A. Puri, *International journal of nanomedicine*, 2015, **10**, 125.
50. S. Punnamaraju, H. You and A. Steckl, *Langmuir*, 2012, **28**, 7657-7664.
51. V. R. Schild, M. J. Booth, S. J. Box, S. N. Olof, K. R. Mahendran and H. Bayley, *Scientific Reports*, 2017, **7**.
52. F. Szoka Jr and D. Papahadjopoulos, *Annual review of biophysics and bioengineering*, 1980, **9**, 467-508.
53. J. D. Berry, M. J. Neesonc, R. R. Dagastineb, D. Y. C. Chanc and R. F. Taborf, *Journal of Colloid and Interface Science*, 2015, **454**, 226-237.
54. G. J. Taylor, G. A. Venkatesan, C. P. Collier and S. A. Sarles, *Soft Matter*, 2015, **11**, 7592-7605.
55. B. A. Heitz, J. Xu, I. W. Jones, J. P. Keogh, T. J. Comi, H. K. Hall Jr, C. A. Aspinwall and S. S. Saavedra, *Langmuir*, 2011, **27**, 1882-1890.
56. M. Makhoul-Mansour, W. Zhao, N. Gay, C. O'Connor, J. Najem, L. Mao and E. C. Freeman, *Langmuir*, 2017.

57. A. Yavlovich, B. Smith, K. Gupta, R. Blumenthal and A. Puri, *Molecular membrane biology*, 2010, **27**, 364-381.

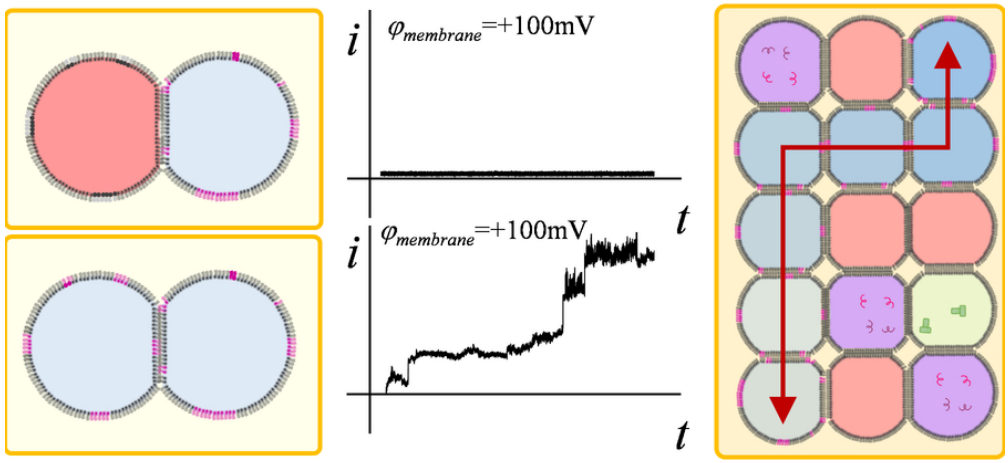

76x36mm (300 x 300 DPI)